Applied Surface Science 370 (2016) 76–82

Contents lists available at ScienceDirect

Applied Surface Science

journal homepage: www.elsevier.com/locate/apsusc

Characterization of the structure, thermal stability and wettability of the TiO_2 nanotubes growth on the Ti–7.5Mo alloy surface

J.M. Chaves [a], A.L.A. Escada [a], A.D. Rodrigues [b], A.P.R. Alves Claro [a,*]

[a] UNESP – Univ. Estadual Paulista, Materials and Technology Department, Faculty of Engineering Guaratinguetá, CEP 12516-410, Guaratinguetá, SP, Brazil
[b] Department of Physics, Federal University of São Carlos, CEP 13565-905, São Carlos, SP, Brazil

ARTICLE INFO

Article history:
Received 5 September 2015
Received in revised form 28 January 2016
Accepted 1 February 2016
Available online 3 February 2016

Keywords:
TiO_2 nanotubes
Ti–7.5Mo alloy
Phase transformation
Average size crystallite

ABSTRACT

In this study, the Ti–7.5Mo experimental alloy for biomedical applications was processed showing orthorhombic (α″) martensite phase and low elastic modulus (54 GPa). The surface treatment permitted the growth of ordered TiO_2 nanotubes via anodization process. The heat treatment during in situ Raman measurement revealed that the TiO_2 nanotubes were transformed of the amorphous state for crystalline (anatase phase) around 400 °C. Annealing of the nanotubes was evaluated by XRD, SEM and Raman spectroscopy. Results showed a high stability of the nanostructure, since only for temperatures above of 500 °C, at which the phase rutile appears, the nanostructure tends to vanish. It was observed in Raman analysis an increasing of the average size of the crystallite of the anatase phase with annealing temperature ranging from 6.5 nm up to 13 nm, besides of the precipitation of the layer rutile in the interface nanotubes–substrate. It is believed that the contact between anatase crystallites or layer rutile of the interface lead to growth of the rutile phase, causing coalescence and subsequent collapse of the tubular nanostructure. The wettability, as well as, surface energy was dependent of the crystalline structure and morphology, becoming more hydrophilic in the anatase phase when as compared with amorphous and rutile phase. The typical features of the surface together excellent bulk properties (low elastic modulus) of the Ti–7.5Mo alloy can provide a guideline for future biomedical applications.

1. Introduction

Titanium dioxide (TiO_2) is among transition-metal oxides most widely studied due to its broad range of functional properties (optical, electronic, chemical, and mechanical) exhibits a large number of applications, including, photocatalysis, energy store, water splitting, gas and humidity sensor, solar cells, electrochromic devices, self-cleaning and anti-bacterial coatings [1–3]. However, the TiO_2 properties in their conventional state, bulk or powder, can be improved or offer new characteristics if reduced to the nanometer scale, due to high surface/volume ratio.

Based on one-dimensional structure of the carbon nanotubes, which provides outstanding electronic properties, such as, high electron mobility or quantum confinement effects, a very high specific surface area, and yet high mechanical strength [1,4], other materials with nanotubular structure, based in transition-metal oxides, has received considerable attention.

In this sense, nanorods, nanowires and nanotubes of TiO_2 had been produced from different techniques, such as, sol–gel method, hydrothermal process, template assisted process. However, a self-ordered growth with superior control over their nanoscale geometry can be obtained via anodic oxidation. This last process allows control on diameter, wall thickness, length, by tailoring parameters such as, electrolyte composition, applied voltage, temperature, and anodizing time [5].

It is well known that nanotubes produced by anodization process are typically amorphous [6,7]. However, the TiO_2 can be crystallize into three structures, being the rutile (tetrahedral) the most stable phase and the anatase (tetrahedral) and the brookite (orthorhombic) metastable phases, which on heating can be transformed to rutile phase. Thus, for a specific application, although having control over the growth parameters of the nanotubes, factors such as, crystalline structure and stability thermal of the structure must be evaluated. For example, in biomedical applications have been reported [8–10] that lattice features of the anatase phase, may to enhance the growth process of hydroxyapatite; the mixed anatase and rutile phases may enhance the photo-catalytic activity [11,12]; and the rutile phase is preferred in electronic devices [13,14] due to its very high dielectric constant. On the other

* Corresponding author.
E-mail address: rosifini@feg.unesp.br (A.P.R. Alves Claro).

http://dx.doi.org/10.1016/j.apsusc.2016.02.017
0169-4332/

hand, evidences of the effect of the substrate features on phase transformation temperature between the allotropic forms of TiO_2 as well as on morphology of nanotubes have also been reported [15–18].

Since exist a wide versatility on TiO_2 nanotubes, and that, an improved performance can be achieved by manipulation of different parameters, the aim of this work is to characterize the effect of the annealing on morphology, structure, thermal stability, phase transformations and wettability of TiO_2 nanotubes grown on the surface of the experimental Ti–7.5Mo alloy for biomedical applications. The interest in the surface modification of Ti–7.5Mo alloy arises from constants efforts to design new alloys with adequate mechanical and chemical properties, since the current commercial alloys Ti–6Al–4V and Ti-cp, have issues due the higher elastic modulus values (~110 GPa) as compared to bone human (10–30 GPa), as well, the presence of harmful ions such as Al and V which are frequently linked to Alzheimer disease and infections.

2. Experimental procedure

Ingots of Ti–7.5Mo alloy (wt.%) were produced in an arc melting furnace under inert atmosphere. These were remelted five times at least to ensure compositional homogeneity. The ingots were submitted to heat treatment at 950 °C for 24 h under vacuum, cold-worked by swaging producing rods with 8 mm of diameter. It was then measured the elastic modulus on plates Ti–7.5Mo alloy using the impulse excitation technique in the flexural configuration. The principle of detection of this equipment is described in the previous paper [19].

Discs of 4 mm thickness were obtained and after polishing and ultrasonic cleaning were used as substrates for growing TiO_2 nanotubes. TiO_2 nanotubes (TNT) were produced by anodization process, at room temperature, with a constant potential of 20 V during 24 h in an electrolyte containing glycerol (90%) in combination with ammonium fluoride (2.5 g NH_4F) and water (10%). In order to promote the amorphous–anatase–rutile transition of TiO_2 nanotubes, samples were annealed in air at different temperatures: 200 °C, 400 °C, 450 °C, 500 °C, 600 °C and 800 °C for 1 h. The samples annealed were denoted as TNT-200, TNT-400, TNT-450, TNT-500, TNT-600, and TNT-800, respectively.

The surface morphologies of the samples were characterized by scanning electronic microscopy (SEM) using FEI Magellan 400L. TiO_2 nanotubes structure was evaluated by X-ray diffraction (XRD), in a Rigaku Rotaflex RU200B equipment, using Cu-Kα radiation (λ = 1.54056 Å). Vibrational characteristics were investigated by Raman spectroscopy. The spectra were collected under ambient conditions by a triple grating Jobin-Yvon T64000 spectrometer, using the line 514.5 nm of an Ar^+ laser as excitation source. The scattered light was collected in a backscattering configuration with a spectral resolution of 2.0 cm^{-1}.

Surface wettability characteristics were evaluated by contact angle measurements using the sessile drop technique, in a goniometer CAM-101 KSV Instruments, equipped with camera for capturing video with 60 s recording interval. From the drop profile of distilled water on the substrate, the software is responsible for determining the contact angle between the two surfaces. The experiments were performed in ambient conditions, taking the mean value of four measurements, at different places on the samples. Additionally, distilled water (polar liquid) and diiodomethane (apolar liquid) were used as test fluids whose surface energy is well-defined. Based on the surface energy parameters of these different liquids, the surface energy was calculated according to Owens–Wendt model, as implemented in software of the equipment. From 3D resolved images of the sample surface, obtained with an objective magnification 100× in a LEXT OLS4100 3D measuring laser microscope, was estimated the average roughness of the samples.

3. Results and discussion

Fig. 1(a) shows the morphology of the Ti–7.5Mo alloy, which exhibits an acicular microstructure typical of orthorhombic martensitic phase (α″), that is consistent with the XRD pattern of Fig. 1(b). In this way, is observed that the wt.% Mo and quenching process from β phase field was sufficient for retain α″ phase at room temperature, as suggested in the literature [20]. The elastic modulus obtained from impulse excitation technique in the flexural configuration was 54 ± 4 GPa at room temperature, which is a good low value for a Ti alloy free of toxic elements as compared with current commercial alloys.

After anodization process, highly ordered and vertically aligned and homogeneous nanotubes were produced on surface of Ti–7.5Mo alloy as observed in Fig. 2. From micrographs obtained by SEM, the inner diameter and mean length of nanotubes were estimated as 65 nm and 500 nm, respectively.

In order to study the structural characteristics of the TiO_2 nanotubes, in situ Raman measurements were accomplished with the sample temperature changing since room temperature (RT) until 630 °C, the spectra collected are shown in Fig. 3.

Fig. 3 shows the amorphous nature of TiO_2 nanotubes in the as-anodized condition (TNT-AC), which was held below of 400 °C. The lack of crystallinity of the amorphous state in the Raman spectra is associated to weak and broad peaks. Above 400 °C are observed changes in the Raman spectra, since appears a sharp peak around

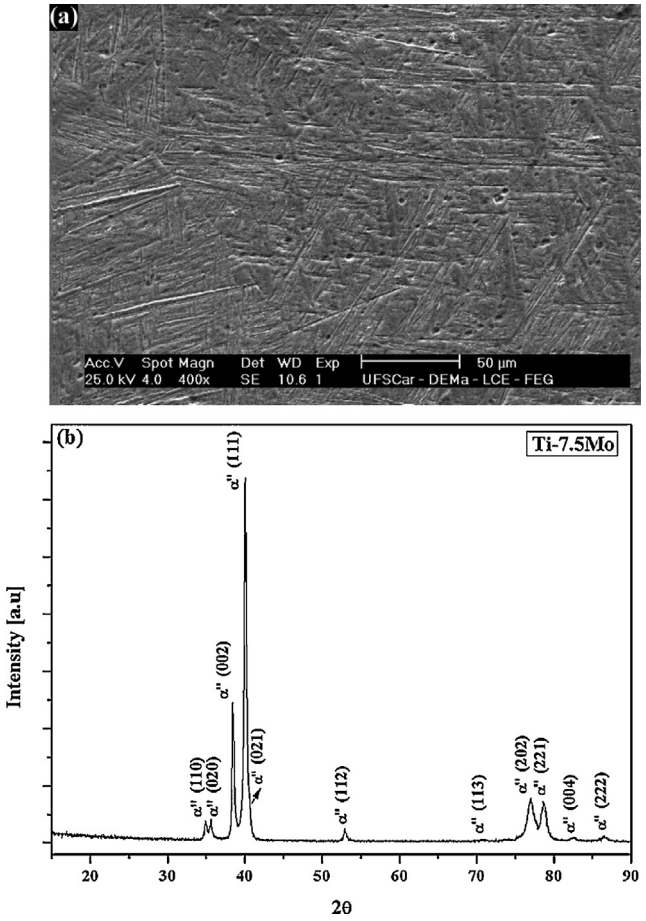

Fig. 1. (a) SEM micrograph and (b) XRD pattern of Ti–7.5Mo alloy used as substrate for growth of TiO_2 nanotubes.

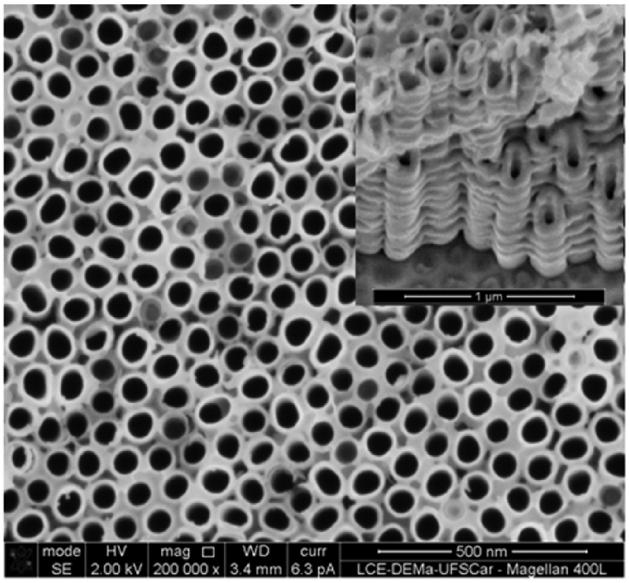

Fig. 2. SEM micrographs showing the nanotubular structure of TiO_2 nanotubes in the as anodization condition (TNT-AC). Inset: cross section view.

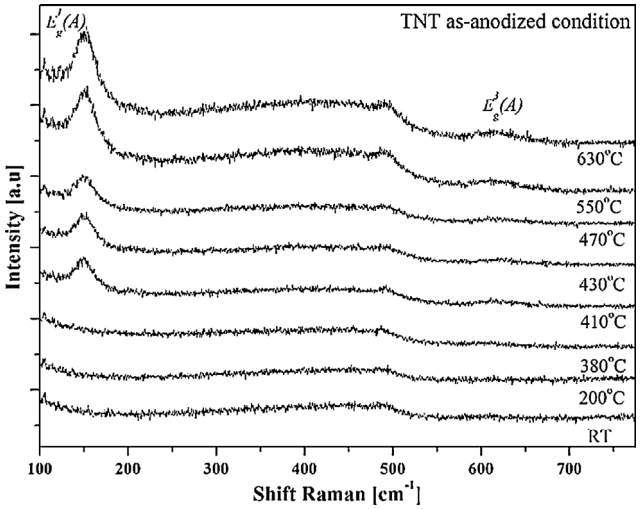

Fig. 3. In situ Raman spectra of TiO_2 nanotubes in the as-anodized condition, collected during heating from room temperature (RT) to 630 °C.

146 cm^{-1}, corresponding to E_g^1 vibration mode, associated to the symmetric stretching vibration of O–Ti–O of the anatase structure [21].

Anatase phase is stable in the full range of temperature studied and it can be observed that, whereas as the temperature is increased, the peak becomes more intense. The increase in the peak intensity may be attributed to the increase in the crystallinity, this fact is consistent with another peak observed around 613 cm^{-1}, corresponding to E_g^2 vibration mode. Thus, from in situ Raman spectra, was showed that the minimum temperature to induce the phase transformation, amorphous–anatase of the TiO_2 nanotubes is around 400 °C.

The structural stability of the TiO_2 nanotubes was studied in samples annealed in the temperature range between 200 °C and 800 °C, during 1 h with heating rate 5 °C/min. The surface morphology of samples after annealing is shown in Fig. 4.

In general, from Fig. 4 could be observed a highly stable nanotubular structure. For samples annealed at 200 °C and 400 °C no changes was observed in the microstructure. During annealing between 450 °C and 500 °C, the precipitates formation leads to close some nanotubes. This behavior is more evident for sample annealed at 600 °C, where part of the nanotubular structure has collapsed. Finally, by annealing at 800 °C the formation of nanoparticles takes place and as consequence the nanotubular structure vanishes being formed a film bulk, as observed in the inset of Fig. 4(f). Insets in Fig. 4 also show that the nanotube–substrate interface, the

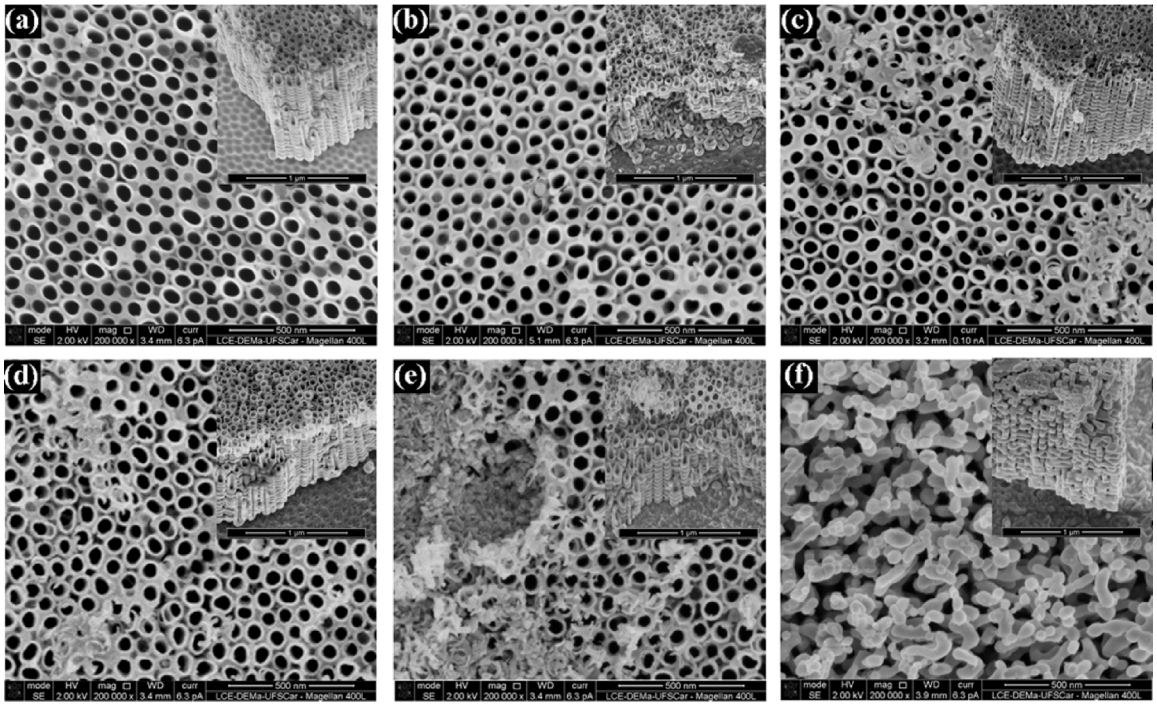

Fig. 4. SEM images of top view of TiO_2 nanotubes annealed at (a) 200 °C, (b) 400 °C, (c) 450 °C, (d) 500 °C, (e) 600 °C and (f) 800 °C. Inset: cross section view of a scratched region.

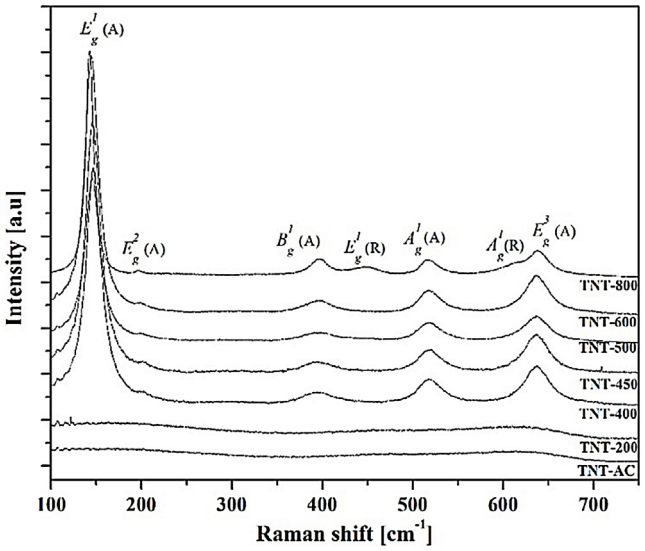

Fig. 5. Raman spectra of TNT anodized and annealed at temperatures between 200 °C and 800 °C, showing the evolution phases, anatase (A) and rutile (R).

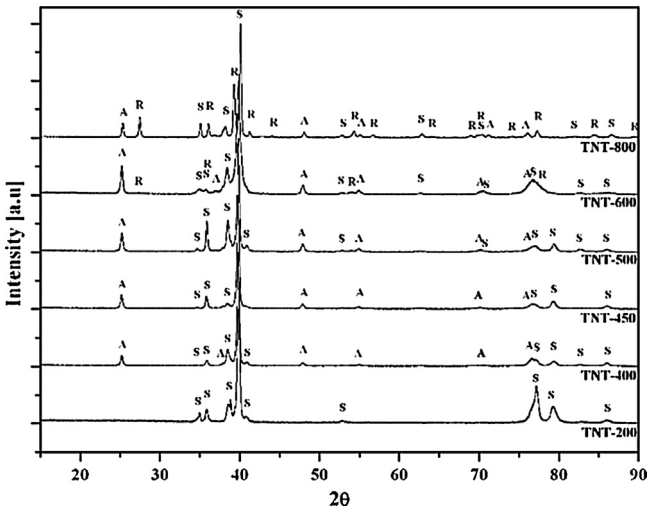

Fig. 6. XRD pattern of TNT anodized and annealed at temperatures between 200 °C and 800 °C, showing the evolution phases, anatase (A) and rutile (R), as well as, peaks related to the substrate (S). It is worth noting that for temperatures above 450 °C occurs changes on substrate, and peaks related to the α-phase of hexagonal structure appear.

dimpled structure on metal surface formed by the rounded bottoms of the nanotube was modified by the annealing treatment.

In the Raman spectra, Fig. 5, is possible to observe that the lack of crystallinity of the amorphous state is held up to 200 °C, this behavior is also showed in the XRD pattern, Fig. 6, since, only peaks related to substrate are observed. For 400 °C the amorphous–anatase phase transformation is evident. This fact was identified in the Raman spectrum for TNT-400 sample, by a sharp peak at 147 cm^{-1}, as well as, peaks at 192 cm^{-1}, 395 cm^{-1}, 516 cm^{-1} and 634 cm^{-1} associated to E_g^1, E_g^2, B_g^1, A_g^1, and E_g^3 vibrations modes characteristics of the anatase phase, respectively. This phase was also identified by diffraction peaks in the XRD pattern, being the most intense around 25° associated to (101) diffraction plane. In general, in Raman spectra, the E_g mode is mainly caused by the symmetric stretching vibration of O–Ti–O in TiO_2, the B_g^2 mode is caused by symmetric bending vibration of O–Ti–O, and the A_g^1 mode is caused by anti-symmetric bending vibration of O–Ti–O [21].

As increase of the temperature, the anatase phase is held up to 500 °C. XRD pattern for TNT-600 sample shows an anatase–rutile mixed phase. This transformation is more evident in the TNT-800 sample, since, the diffraction peaks associated to rutile phase are displayed, while the most intense diffraction peak vanishes. The detection of the rutile phase in the Raman spectrum is given by the presence of the E_g^1 vibration mode, in 446 cm^{-1}, and a shoulder around 610 cm^{-1}, corresponding to A_g^1 vibration mode (Fig. 5).

An analysis more detailed of XRD patterns (Fig. 6), shows as with increasing of the temperature, the intensity of (101) diffraction peak is increased. Also an interesting effect can be notice in the lowest energy range of the Raman spectra (Fig. 5). With increasing of the annealing temperature, the peak at around 147 cm^{-1} related to E_g^1 mode, progressively shifts to higher energies and become broader. Fig. 7(a) shows the Raman spectra of the samples annealed at 400 °C, 600 °C and 800 °C, in which the differences in both energy and breadth can be clearly noticed. Fig. 7(b) shows the decrease of the central position and of the full width at half maximum (FWHM) of the peak E_g^1 with the increasing of temperature.

These changes in the central position and width of Raman peaks can be associated to an increasing in the average size of the crystallites in the nanotubes. For phonons propagating in perfect and infinite crystals, the momentum conservation requires that only phonons with momenta lying near Brillouin zone center ($q \sim 0$) participates in Raman scattering, resulting in a sharp symmetrical peak. When we are dealing with small crystallites, the phonon propagation describes a finite correlation length with dimensions of the same order as the crystallites sizes, leading to a relaxation of selection rule for phonon momenta. Since E_g^1 vibrational

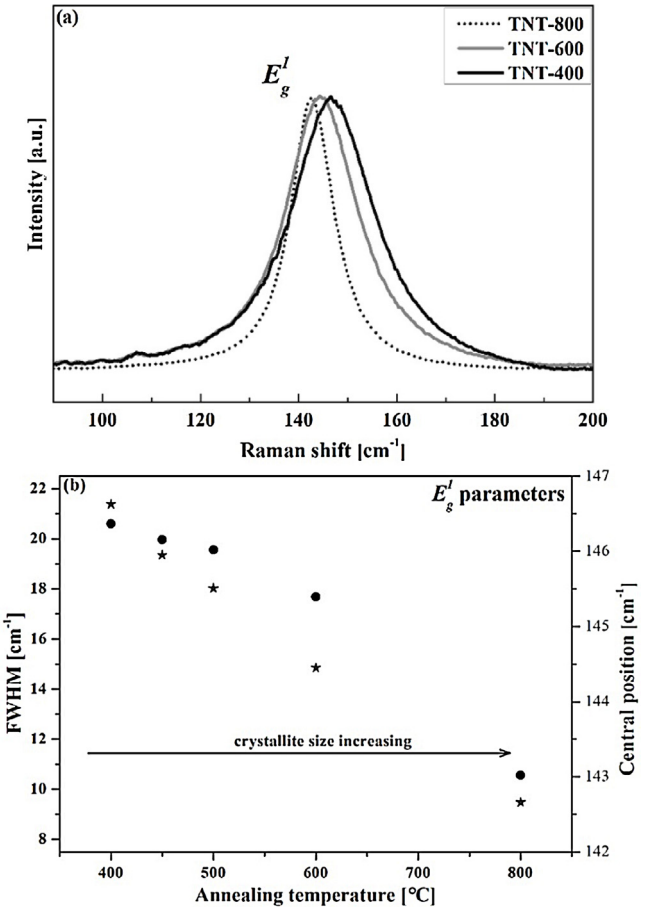

Fig. 7. (a) Raman spectra taken from TiO_2 nanotubes annealed at different temperatures. (b) Central position (stars) and full width at half maximum (circles) of E_g^1 peak as a function of annealing temperature.

mode presents a positive dispersion relation, phonons with higher wavenumbers will participate of the Raman scattering, resulting in a peak with upward asymmetric shape. The smaller the crystallite dimensions the broader (and more energetic) the peak. The resulting theoretical Raman intensity can be calculated using the phonon confinement model [22].

By fitting it with the experimental spectra, we have found the dimensions in which the phonons are confined, that correspond approximately to the crystallites size. The method used here is similar to that reported in [23]. As an example of the adopted procedure, Fig. 8(a) shows experimental Raman spectrum of the nanotubes annealed at 800 °C (open circles) and its best fit with the theoretical spectrum (solid line). By performing these calculations with every Raman spectra we have estimated the average crystallite sizes of the anatase phase in the annealed nanotubes. The dispersion relations of E_g^1 phonons of anatase TiO_2 used in our calculations were taken from [24]. The results are shown in Fig. 8(b).

As showed in Fig. 8(b), the annealing treatment led to increasing of the average size crystallite ranging from 6.5 nm up to 13 nm. Indeed this increase on average size crystallite given by the atomic rearrangement during phase transformations, toward an energetically more favorable equilibrium state causes changes on the nanotubes, observing an increase in the wall thickness, as well as, closure of pores and subsequent collapse.

On the other hand, Hardcastle et al. [25] suggested that impurities interstitial and oxygen vacancies in the nanotubes/substrate interface plays an important role during the crystallization and phase transformations of the TiO_2 nanotubes. Since the impurities coming from the reduced states of titanium, increases the number of oxygen vacancies in the nanotube/substrate interface, during annealing, it may be form an oxide layer of rutile phase on interface.

In this sense, an additional characterization obtained by XRD and SEM in the Ti–7.5Mo alloy (Fig. 9(a)), revealed that the heat treatment above 500 °C leads to precipitation of rutile layer, of about 2 μm, on surface of the alloy. A sample with TiO_2 nanotubes and annealed at 500 °C (TNT-500) which was scratched, to permit take off part of the nanotubes of the substrate surface, was analyzed by Raman scattering (Fig. 9(b) and (c)). As expected the Raman spectrum revealed that the oxide layer formed in the interface substrate/nanotube is in the rutile phase.

Thus, the nanotubes in amorphous state transforms to anatase phase and whereas the oxygen diffusion occurs at interface, proceeds the nucleation and growth process. From the work of the Zhang et al. [26], the nucleation of rutile phase could take place at

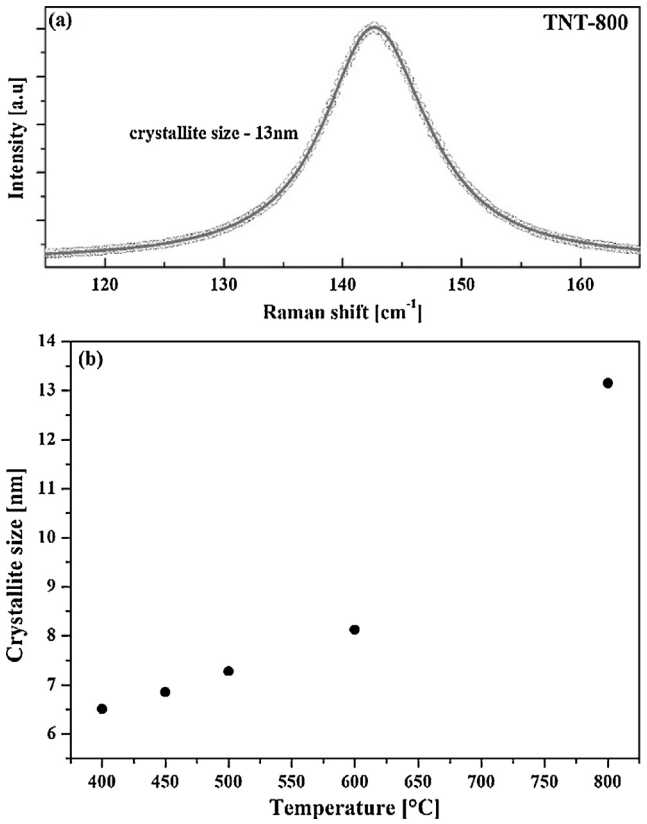

Fig. 8. (a) Experimental Raman data for the sample treated at 800 °C (open circles) and its best fit with the theoretical spectra (solid line). (b) Average crystallite sizes for each sample determined by this technique.

interface of contact between two anatase particles, which results in the transformation of anatase grains into large rutile grain; the growth may happen when rutile crystallites comes into contact with a crystallite of anatase, or when two rutile nuclei emerge together [26].

Herein, the annealing increase the crystallites size of the anatase phase, as observed in Fig. 8(b), and since these come in contact with each other or with rutile crystals at the interface, occurs the anatase–rutile phase transformation in the nanotubes. So, with growth rutile crystals start the coalescence and the tubular

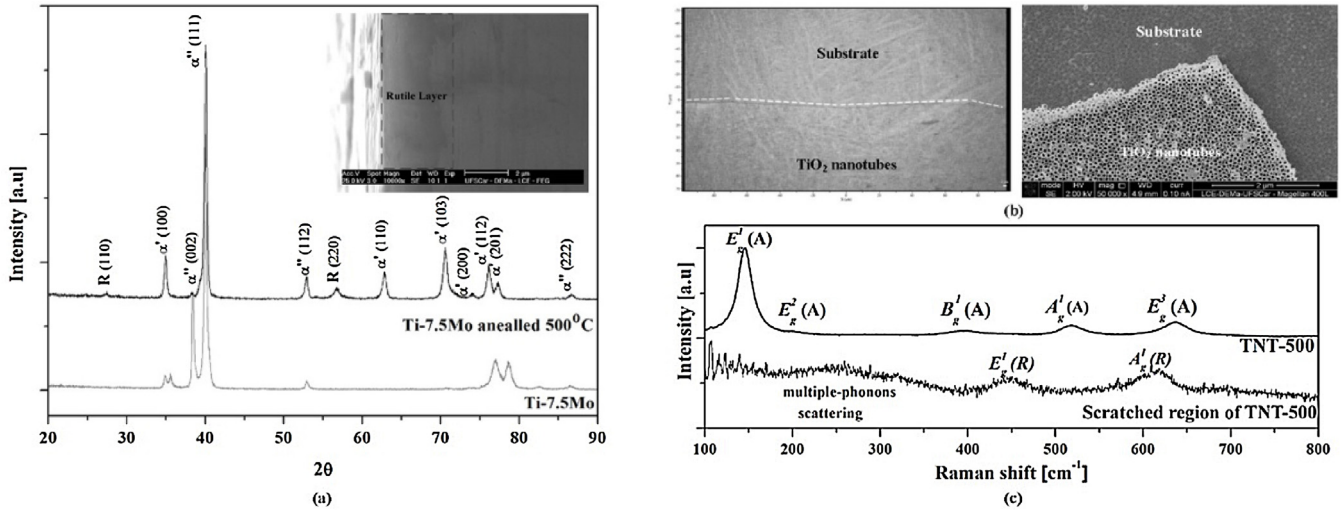

Fig. 9. Precipitation of layer rutile in: (a) Ti–7.5Mo alloy annealed 500 °C showed from XRD and SEM analysis; (b) interface substrate/nanotube showed the scratched region of the TNT-500 sample obtained by optical and scanning electronic microscopy; and (c) comparative Raman spectrum of TNT-500 and scratched region.

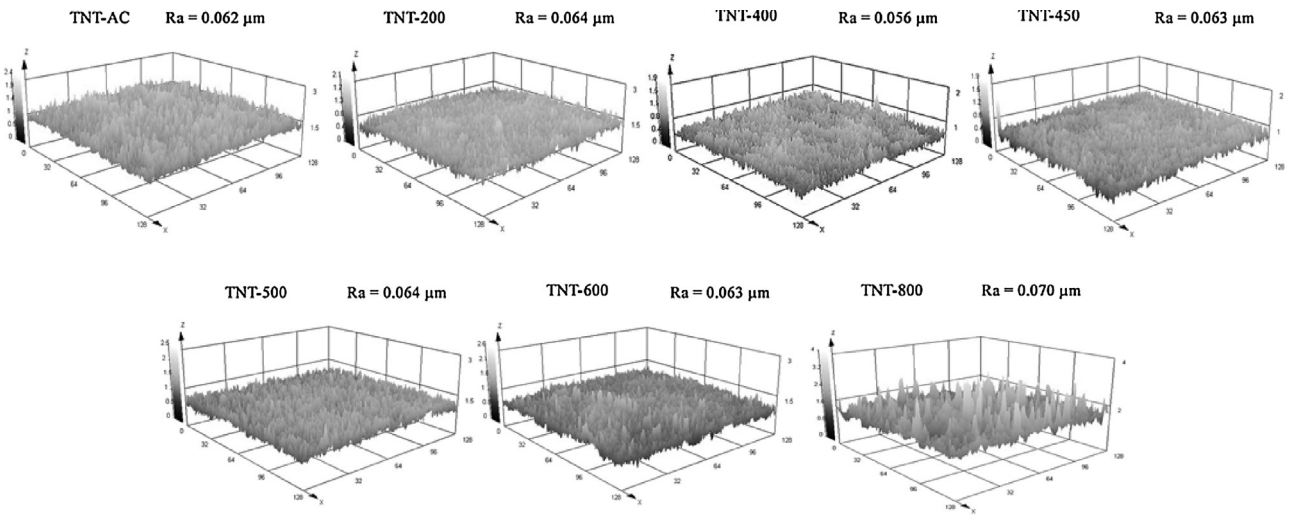

Fig. 10. Representative surface images and average roughness values (*Ra*) of TNT anodized and annealing at temperatures between 200 °C and 800 °C.

nanostructure tends to vanish. As the rutile phase spread out into the nanotubes, the collapse of the tubular nanostructure is expected and a dense rutile film is observed.

On the other hand, it is well known that wettability, which may be studied by water contact angle (WCA) measurements, of thin films can be influenced by the processing method and heat treatment, which modifies the chemical and physical properties. Thus, to WCA < 90° the surface is considered hydrophilic, whereas WCA > 90° the surface is hydrophobic.

In order to study the annealing effect on wettability of the TiO_2 nanotubes, were carried out measures of contact angle, surface energy (γ) and average roughness (*Ra*), the results are summarized in Fig. 10 and Table 1. In general, the changes showed in the contact angle, γ and *Ra*, may depend on the crystalline structural and surface morphology of the film. Evidences of these dependencies were recently observed, such as, more hydrophilic surfaces (contact angle lower to 40°) in samples with 300 nm length nanotubes [6]; pH and electrolyte bath conditions may vary the length and modifies the presence of lattice imperfections in the anatase phase, which affect the surface energy and contact angle [27].

Samples with TiO_2 nanotubes in the amorphous state showed higher contact angle values, which are related to hydrophobic behavior. It was found that annealing treatment affect this behavior, making the surface more hydrophilic in the samples with nanotubes in anatase phase (TNT-400 and TNT-450), since there was a decreasing on contact angle values. This fact, can be associated to the chemisorbed hydroxyl groups as result of the anodization process, which favors the formation of the hydrogen bonds on surface [28] and so makes the surface with high superficial activity, as observed by the γ values in Table 1.

Table 1
Contact angle and surface energy values of TNT anodized and annealed at temperatures between 200 °C and 800 °C.

Sample	Contact angle (°)		Surface energy (mJ/m^2)
	DI water	Diidomethane	
TNT-AC	116.3 ± 1.6	93 ± 1.9	49.2 ± 2.3
TNT-200	118.5 ± 1.9	84 ± 2.1	50.12 ± 2.8
TNT-400	76.2 ± 1.4	67 ± 1.8	72.84 ± 2.1
TNT-450	58.1 ± 2.1	52 ± 2.6	93.15 ± 2.5
TNT-500	68.6 ± 2.6	73 ± 1.4	83.77 ± 1.8
TNT-600	99.8 ± 1.8	87 ± 2.3	57.32 ± 2.5
TNT-800	80.6 ± 2.3	71 ± 1.6	65.28 ± 2.6

As increase the annealing temperature, the anatase–rutile phases coexist and the contact angle values again increased (γ decrease), lowering the hydrophilic behavior. In this case, the loss of the hydrophilicity for the samples annealed above 500 °C, could be due to growth of the rutile phase that break the nanostructure. It might so the surface become irregular and take off film of the substrate, retaining air inside, which prevents the liquid permeates the surface. When the sample was annealed at 800 °C, and the nanostructure collapses completely forming a dense rutile film, occurs a new reduction on contact angle value accompanied with a slight increase of γ values. The *Ra* values shown a roughness profile homogenous with a mean value of about 0.063 μm in the samples with nanotubes, while, in the sample annealed at 800 °C a slight change on roughness profile (*Ra* = 0.070 μm) is qualitatively observed which may be due to dense rutile film formed.

These results shown that the surface modification of the Ti–7.5Mo alloy by growth TiO_2 nanotubes and subsequent annealing treatment, that lead to changes on crystallinity and morphology of the TiO_2 nanotubes, influences its hydrophilic behavior. So the following directions for future research will seek evaluate its biological response, since as reported in literatures [29,30] the human bone cell interaction is dependent on surface morphology.

4. Conclusions

In summary, TiO_2 nanotubes highly ordered, vertically aligned and homogeneously distributed were grown on surface Ti–7.5Mo alloy, which is attractive for applications, such as, metallic alloys for biomedical implants, in view of lower elastic modulus and composition free toxic elements.

TiO_2 nanotubes presented high thermal stability, since on annealing between 400 °C and 450 °C, temperature in which the transformation amorphous–anatase occurs, the surface morphology remains uniform. For temperature above 500 °C, with the growth of the anatase crystallites and the oxidation in the interface, nanotubes/substrate, is induced the anatase–rutile transformation, that leads to coalescence of the nanostructure with subsequent collapse after growth of the rutile phase. TiO_2 nanotubes presented a wettability and surface energy dependent on crystalline structure and morphology, since TiO_2 nanotubes in the anatase phase, becoming more hydrophilic, as compared with amorphous and rutile phase.

Whereas that the biological responses of the biomaterials, such as, protein adsorption, adhesion and proliferation cellular

is dependent on surface features, the results indicate that surface modification of the Ti–7.5Mo alloy, may have characteristics that satisfy these requirements. Studies in regarding to biological behavior are ongoing and will be discussed in ongoing future publications.

Acknowledgments

The authors gratefully acknowledge the Brazilian Research Funding Agencies, National Council for Scientific and Technological Development (CNPq) (Research Grant 486352/2013-7 and Grant 501465/2012-0), State of São Paulo Research Foundation (FAPESP) (Grant 2013/08200-9) for their financial support of this work.

References

[1] P. Roy, S. Berger, P. Schmuki, TiO_2 nanotubes: synthesis and applications, Angew. Chem. 50 (2011) 2904–2939.
[2] C.A. Grimes, Synthesis and application of highly ordered arrays of TiO_2 nanotubes, J. Mater. Chem. 17 (2007) 1451.
[3] A. Ghicov, P. Schmuki, Self-ordering electrochemistry: a review on growth and functionality of TiO_2 nanotubes and other self-aligned MO(x) structures, Chem. Commun. (2009) 2791–2808.
[4] C.N.R. Rao, A.M. Müller, A.K. Cheetham, The Chemistry of Nanomaterials: Synthesis, Properties and Applications, Wiley-VCH, Weinheim, Germany, 2006.
[5] C.A. Grimes, G.K. Mor, TiO_2 Nanotube Arrays Synthesis, Properties, and Applications, Springer, 2009.
[6] A. Shivaram, S. Bose, A. Bandyopadhyay, Thermal degradation of TiO_2 nanotubes on titanium, Appl. Surf. Sci. 317 (2014) 573–580.
[7] D. Fang, Z. Luo, K. Huang, D.C. Lagoudas, Effect of heat treatment on morphology, crystalline structure and photocatalysis properties of TiO_2 nanotubes on Ti substrate and freestanding membrane, Appl. Surf. Sci. 257 (2011) 6451–6461.
[8] M. Uchida, H.-M. Kim, T. Kokubo, S. Fujibayashi, T. Nakamura, Structural dependence of apatite formation on titania gels in a simulated body fluid, J. Biomed. Mater. Res. A 64A (2003) 164–170.
[9] A.L. Escada, J.P. De Barros Machado, R. Nakazato, A.P. Alves Claro, Deposition of calcium phosphate coating on TiO_2 nanotube arrays, Dent. Mater. 29 (Suppl. 1) (2013) e9.
[10] H. Tsuchiya, J.M. Macak, L. Müller, J. Kunze, F. Müller, P. Greil, S. Virtanen, P. Schmuki, Hydroxyapatite growth on anodic TiO_2 nanotubes, J. Biomed. Mater. Res. A 77A (2006) 534–541.
[11] B. Mario, E. Wolfgang, Mixed phase anatase/rutile titanium dioxide nanotubes for enhanced photocatalytic degradation of methylene-blue, Nano-Micro Lett. 3 (2011) 236–241.
[12] L. Pan, H. Huang, C.K. Lim, Q.Y. Hong, M.S. Tse, O.K. Tan, TiO_2 rutile–anatase core–shell nanorod and nanotube arrays for photocatalytic applications, RSC Adv. 3 (2013) 3566–3571.
[13] D. Eder, I.A. Kinloch, A.H. Windle, Pure rutile nanotubes, Chem. Commun. (2006) 1448–1450.
[14] M. Kadoshima, M. Hiratani, Y. Shimamoto, K. Torii, H. Miki, S. Kimura, T. Nabatame, Rutile-type TiO_2 thin film for high-*k* gate insulator, Thin Solid Films 424 (2003) 224–228.
[15] C.P. Ferreira, M.C. Gonçalves, R. Caram, R. Bertazzoli, C.A. Rodrigues, Effects of substrate microstructure on the formation of oriented oxide nanotube arrays on Ti and Ti alloys, Appl. Surf. Sci. 285 (2013) 226–234.
[16] W.-G. Kim, H.-C. Choe, Y.-M. Ko, W.A. Brantley, Nanotube morphology changes for Ti–Zr alloys as Zr content increases, Thin Solid Films 517 (2009) 5033–5037.
[17] S.-H. Jang, H.-C. Choe, Y.-M. Ko, W.A. Brantley, Electrochemical characteristics of nanotubes formed on Ti–Nb alloys, Thin Solid Films 517 (2009) 5038–5043.
[18] H.-C. Choe, W.-G. Kim, Y.-H. Jeong, Surface characteristics of HA coated Ti–30Ta–*x*Zr and Ti–30Nb–*x*Zr alloys after nanotube formation, Surf. Coat. Technol. 205 (2010) S305–S311.
[19] J.M. Chaves, O. Florêncio, P.S. Silva Jr., P.W.B. Marques, C.R.M. Afonso, Influence of phase transformations on dynamical elastic modulus and anelasticity of beta Ti–Nb–Fe alloys for biomedical applications, J. Mech. Behav. Biomed. Mater. 46 (2015) 184–196.
[20] W.F. Ho, C.P. Ju, J.H. Chern Lin, Structure and properties of cast binary Ti–Mo alloys, Biomaterials 20 (1999) 2115–2122.
[21] J. Yan, G. Wu, N. Guan, L. Li, Z. Li, X. Cao, Understanding the effect of surface/bulk defects on the photocatalytic activity of TiO_2: anatase versus rutile, Phys. Chem. Chem. Phys. 15 (2013) 10978–10988.
[22] I.H. Campbell, P.M. Fauchet, The effects of microcrystal size and shape on the one phonon Raman spectra of crystalline semiconductors, Solid State Commun. 58 (1986) 739–741.
[23] S. Balaji, Y. Djaoued, J. Robichaud, Phonon confinement studies in nanocrystalline anatase-TiO_2 thin films by micro Raman spectroscopy, J. Raman Spectrosc. 37 (2006) 1416–1422.
[24] M. Mikami, S. Nakamura, O. Kitao, H. Arakawa, Lattice dynamics and dielectric properties of TiO_2 anatase: a first-principles study, Phys. Rev. B 66 (2002) 155213.
[25] F.D. Hardcastle, H. Ishihara, R. Sharma, A.S. Biris, Photoelectroactivity and Raman spectroscopy of anodized titania (TiO_2) photoactive water-splitting catalysts as a function of oxygen-annealing temperature, J. Mater. Chem. 21 (2011) 6337.
[26] H. Zhang, J.F. Banfield, Phase transformation of nanocrystalline anatase-to-rutile via combined interface and surface nucleation, J. Mater. Res. 15 (2000) 437–448.
[27] B. Munirathinam, H. Pydimukkala, N. Ramaswamy, L. Neelakantan, Influence of crystallite size and surface morphology on electrochemical properties of annealed TiO_2 nanotubes, Appl. Surf. Sci. 355 (2015) 1245–1253.
[28] D.H. Shin, T. Shokuhfar, C.K. Choi, S.-H. Lee, C. Friedrich, Wettability changes of TiO_2 nanotube surfaces, Nanotechnology 22 (2011) 315704.
[29] K. Das, A. Bandyopadhyay, S. Bose, Biocompatibility and in situ growth of TiO_2 nanotubes on Ti using different electrolyte chemistry, J. Am. Ceram. Soc. 91 (2008) 2808–2814.
[30] K. Das, S. Bose, A. Bandyopadhyay, TiO_2 nanotubes on Ti: influence of nanoscale morphology on bone cell–materials interaction, J. Biomed. Mater. Res. A 90 (2009) 225–237.